

Journal of Materials Chemistry C

Accepted Manuscript



This is an *Accepted Manuscript*, which has been through the Royal Society of Chemistry peer review process and has been accepted for publication.

Accepted Manuscripts are published online shortly after acceptance, before technical editing, formatting and proof reading. Using this free service, authors can make their results available to the community, in citable form, before we publish the edited article. We will replace this *Accepted Manuscript* with the edited and formatted *Advance Article* as soon as it is available.

You can find more information about *Accepted Manuscripts* in the [Information for Authors](#).

Please note that technical editing may introduce minor changes to the text and/or graphics, which may alter content. The journal's standard [Terms & Conditions](#) and the [Ethical guidelines](#) still apply. In no event shall the Royal Society of Chemistry be held responsible for any errors or omissions in this *Accepted Manuscript* or any consequences arising from the use of any information it contains.

ARTICLE

White light Emission of IFP-1 by In-situ Co-doping of the MOF Pore System with Eu^{3+} and Tb^{3+}

Cite this: DOI: 10.1039/x0xx00000x

Suvendu Sekhar Mondal,^a Karsten Behrens,^a Philipp R. Matthes,^b Fabian Schönfeld,^b Jörn Nitsch,^b Andreas Steffen,^b Philipp-Alexander Primus,^c Michael U. Kumke,^c Klaus Müller-Buschbaum^{*,b} and Hans-Jürgen Holdt^{*,a}

Received 00th January 2012,

Accepted 00th January 2012

DOI: 10.1039/x0xx00000x

www.rsc.org/

Co-doping of the MOF $^3_\infty[\text{Zn}(2\text{-methylimidazolate-4-amide-5-imidate})]$ (IFP-1 = Imidazolate Framework Potsdam-1) with luminescent Eu^{3+} and Tb^{3+} ions presents an approach to utilize the porosity of the MOF for the intercalation of luminescence centers and for tuning of the chromaticity to the emission of white light of the quality of a three color emitter. Organic based fluorescence processes of the MOF backbone as well as metal based luminescence of the dopants are combined to one homogenous single source emitter while retaining the MOF's porosity. The lanthanide ions Eu^{3+} and Tb^{3+} were doped in-situ into IFP-1 upon formation of the MOF by intercalation into the micropores of the growing framework without a structure directing effect. Furthermore, the color point is temperature sensitive, so that a cold white light with a higher blue content is observed at 77 K and a warmer white light at room temperature (RT) due to reduction of the organic emission at higher temperatures. The study further illustrates the dependence of the amount of luminescent ions on porosity and sorption properties of the MOF and proves the intercalation of luminescence centers into the pore system by low-temperature site selective photoluminescence spectroscopy, SEM and EDX. It also covers an investigation on the border of homogenous uptake within the MOF pores and formation of secondary phases of lanthanide formates on the surface of the MOF. Crossing the border from a homogenous co-doping to a two-phase composite system can be beneficially used to adjust the character and warmth of the white light. This study also describes two-color emitters of the formula $\text{Ln}@IFP-1a-d$ (Ln: Eu, Tb) by doping with just one lanthanide Eu^{3+} or Tb^{3+} .

1 Introduction

Metal Organic Frameworks (MOFs) with interesting photophysical properties contribute to the overall variety of functionality of these inorganic organic hybrid materials.¹⁻⁶ MOFs can show effective luminescence by organic chromophore based fluorescence as well as by metal based luminescence processes.⁷ This includes different energy transfer mechanisms between linker ligands and metal centers.⁸ Similar to today's phosphor converted LED phosphors, co-doping of host lattices with lanthanide ions can be utilized to set a defined amount of luminescence centers in the hybrid material.⁹ For a MOF this can in principle be achieved by replacement of the connectivity centers of the framework or by intercalation into cavities of the porous MOF lattice. The choice of the luminescence centers can be used to set the color point of the resulting phosphor. Deliberate choice and mixing of dopants open a path to tune the color point of the material up to

the stage of the emission of white light, as shown for SMOF-1, $\text{In}(\text{BTB})_{2/3}(\text{OA})(\text{DEF})_{3/2}$ co-doped with Eu^{3+} (Sandia Metal-Organic Framework-1, BTB: 1,3,5-tris(4-carboxyphenyl)benzene, OA: oxalic acid, DEF: *N,N'*-diethylformamide).¹⁰ Today, several approaches for color tuning and white emitting coordination polymers and MOFs have been published.¹¹ Due to the requirement of a combination of different luminescent species in one homogenous compound to emit white light, each of these white emitters has been a significant step forward. They exhibit different strategies to achieve white light: co-doping with luminescent metal ions by replacement of the connectivity centers of the framework or coordination polymer,^{11a,b} a controlled setting of metal positions in bimetallic compounds for Ag and Eu,^{11c} or a functionalization of pore walls for excitation dependent light emission.^{11d} A utilization of the pore system of the MOF for white light emission was achieved by implementing emitting Ir-complexes $[\text{Ir}(\text{ppy})_2(\text{bpy})]^{+11e}$ as well as luminescent lanthanide

ions.^{11c} The influence of these procedures on the porosity of the material after filling the pores has not yet been reported. In order to build luminescent functional MOFs synthetic approaches have been developed and such functional MOFs were reviewed recently.⁸ The creation of white light has been elaborated by scientists and technicians for a long time with the temperature of the white tone being decisive for the acceptance of new lighting devices and thus the introduction of new technologies.¹² In today's LEDs color mixing by a combination of phosphors (including color converted LED phosphors) is used to set the chromaticity and thus the color point of a light emitter.¹³

We have previously developed a class of metal imidazolate-4-amide-5-imidates based metal organic frameworks called IFP.¹⁴ As it is known that Eu^{3+} and Tb^{3+} ions emit red and green light, respectively, it can be expected that zinc metal based IFP-1^{14a} co-doped with Eu^{3+} and Tb^{3+} may act as a trichromatic emitter upon retaining the luminescence of all components. Proper mixing can thereby give options for white-light emission. This study reports the solvothermal synthesis of IFP-1 in DMF in the presence of $\text{Eu}(\text{NO}_3)_3 \cdot 6\text{H}_2\text{O}$ and $\text{Tb}(\text{NO}_3)_3 \cdot 5\text{H}_2\text{O}$, at first for one Ln^{3+} ion at a time [named as Ln@IFP-1a-d ($\text{Ln} = \text{Eu}$ or Tb)] to generate two-color emitters exhibiting the MOF backbone and the Ln^{3+} -emission. Co-doping was then expanded to simultaneous use of both, Eu^{3+} and Tb^{3+} [named as EuTb@IFP-1a-d or white light emitter] to create three-color white light emitting materials, respectively. We also elaborated the influence of co-doping on the porosity of the MOF by gas adsorption studies (BET) and investigated the luminescence properties, especially tuning of the chromaticity of the emission including the warmth of white light. Finally, the study also describes the border of homogenous doping of the pore system by formation of lanthanide formats as side phases.

2 Experimental

Materials and Synthesis

Ln^{3+} nitrates [$\text{Eu}(\text{NO}_3)_3 \cdot 5\text{H}_2\text{O}$ 99.99% trace metals basis and $\text{Tb}(\text{NO}_3)_3 \cdot 5\text{H}_2\text{O}$ 99.9% trace metals basis] were used as purchased from Aldrich. DMF was purchased from VWR International. All reagents and solvents were used without further purification.

Synthesis of Ln@IFP-1a-d ($\text{Ln} = \text{Eu}$ or Tb):

$^3_{\infty}[\text{Zn}(\text{2-methylimidazolate-4-amide-5-imidate})_2] \cdot 3\text{H}_2\text{O}$ (IFP-1) was synthesized according to the previously published procedure.^{14a} To get lanthanide co-doped materials, the synthetic procedure was modified. The reaction mixture containing $\text{Zn}(\text{NO}_3)_2 \cdot 4\text{H}_2\text{O}$ (198 mg, 0.76 mmol) and different equivalents of $\text{Eu}(\text{NO}_3)_3 \cdot 6\text{H}_2\text{O}$ or $\text{Tb}(\text{NO}_3)_3 \cdot 5\text{H}_2\text{O}$ (from 0.25 to 1.00 equiv.) and 4,5-dicyano-2-methylimidazole (**1**, 100 mg, 0.76 mmol) were dissolved in DMF (6 mL) in a sealed tube. The tube was closed and the mixture was heated up to 110 °C for 72 h and then cooled to room temperature. Crystalline material was formed, which are addressed to as Ln@IFP-1a-d

in the following report based on molar ratio of lanthanides and the linker precursor (**1**, Scheme 1 and Table 1).

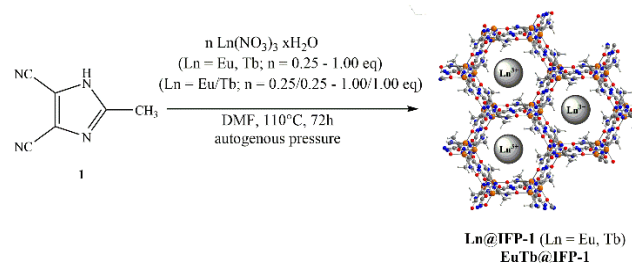
Synthesis of EuTb@IFP-1a-d :

$\text{Tb}(\text{NO}_3)_3 \cdot 5\text{H}_2\text{O}$ (from 0.25/0.25, to 1.00/1.00 equiv.), $\text{Eu}(\text{NO}_3)_3 \cdot 6\text{H}_2\text{O}$ (from 0.25/0.25, to 1.00/1.00 equiv.), $\text{Zn}(\text{NO}_3)_2 \cdot 4\text{H}_2\text{O}$ (198 mg, 0.76 mmol) and 4,5-dicyano-2-methylimidazole (**1**, 100 mg, 0.76 mmol) were dissolved in DMF (6 mL) in a sealed tube. The reaction mixtures were then treated as described above (Scheme 1 and Table 1). Physical characterization of all materials was done by elemental analysis, inductively coupled plasma atomic emission spectroscopy (ICP-OES) and X-ray powder diffraction (PXRD) patterns (see ESI for details). To get activated materials, the as-synthesized samples of Ln@IFP-1 were heated to 200 °C at a vacuum of $1 \cdot 10^{-3}$ mbar for 48 hours to remove remaining DMF and water molecules.

3 Results and discussion

Structure determination

The synthesis of luminescent co-doped MOFs is usually based on the statistic replacement of a certain amount of metal ions as connectivity centers by luminescent ions like Ln^{3+} during MOF formation.⁹ Statistic replacement is thereby fundamentally dependent on a match of the two different metal ions in parameters like ionic radii, valence and chemical reactivity. For a potential co-doping of IFP-1 with lanthanide ions, these parameters do not match with Zn^{2+} .¹⁵ Accordingly, also options like the formation of heterobimetallic compounds or the utilization of the pore system had to be investigated. On the other hand, the approach of in-situ ligand synthesis simultaneous to the MOF formation seemed promising to immobilize highly charged ions within the pore system and to thereby avoid a postsynthetic treatment hindered by electrostatic interactions. For the intercalation of lanthanide ions into the MOF pores, the solvothermal reactions of the linker-precursor 4,5-dicyano-2-methylimidazole (**1**) and $\text{Zn}(\text{NO}_3)_2 \cdot 4\text{H}_2\text{O}$ were carried out together with different equivalents of nitrates of europium and terbium (Scheme 1 and Table 1).



Scheme 1. In-situ synthesis of single co-doped Eu@IFP-1a-d , Tb@IFP-1a-d and double co-doped EuTb@IFP-1a-d .

Table 1. Eu- and Tb-single co-doped as well as EuTb-double co-doped IFP-1 samples (all activated) measured by ICP-OES.

IFP-1 material co-doped with lanthanides	Equivalents of		atom% (product) ^{b)}		
	Eu(NO ₃) ₃ ·6H ₂ O ^{a)}	Tb(NO ₃) ₃ ·5H ₂ O ^{a)}	Eu	Tb	Zn
Eu@IFP-1a	0.25		0.02 ± 0.01		99.98 ± 0.01
Eu@IFP-1b	0.50		0.03 ± 0.02		99.97 ± 0.02
Eu@IFP-1c	0.75		0.48 ± 0.06		99.52 ± 0.06
Eu@IFP-1d	1.00		1.04 ± 0.06		98.96 ± 0.06
Tb@IFP-1a		0.25		0.07 ± 0.02	99.93 ± 0.02
Tb@IFP-1b		0.50		0.11 ± 0.01	99.89 ± 0.01
Tb@IFP-1c		0.75		0.10 ± 0.03	99.90 ± 0.03
Tb@IFP-1d		1.00		0.16 ± 0.01	99.84 ± 0.01
EuTb@IFP-1a	0.25	0.25	0.04 ± 0.02	0.04 ± 0.01	99.93 ± 0.03
EuTb@IFP-1b	0.50	0.50	0.10 ± 0.03	0.11 ± 0.02	99.80 ± 0.05
EuTb@IFP-1c	0.75	0.75	0.91 ± 0.56	0.91 ± 0.54	98.18 ± 1.10
EuTb@IFP-1d	1.00	1.00	7.16 ± 0.24	6.76 ± 0.19	86.07 ± 0.42

a) Referred to the equivalents of Zn(NO₃)₂·4H₂O employed in the synthesis; b) atom%, referred to the metal content; determined by ICP-OES.

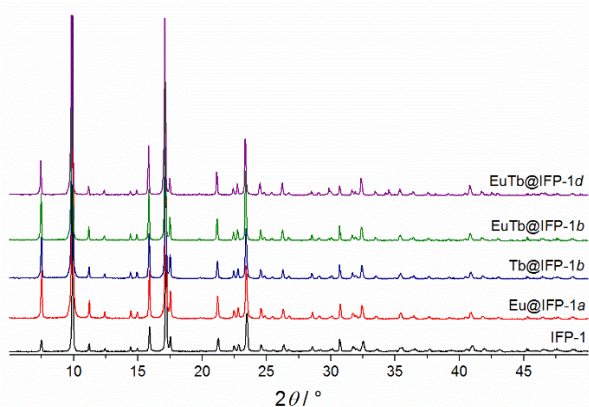


Fig. 1 X-ray powder diffraction patterns of Ln@IFP-1; Cu-K_α radiation ($\lambda=1.54056 \text{ \AA}$).

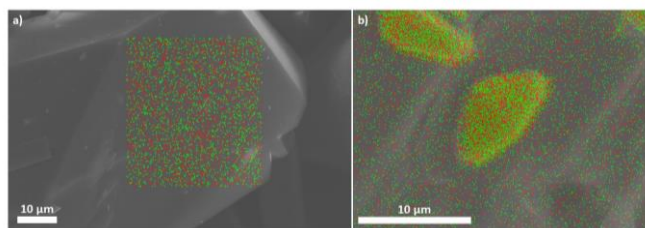


Fig. 2 Eu(red)- and Tb(green)-elemental mapping of a) of EuTb@IFP-1b and b) EuTb@IFP-1d.

The Ln@IFP-1a - d (Ln = Eu or Tb) and EuTb@IFP-1a - d with amounts of lanthanides up to 14.0 atom% display the PXRD patterns identical IFP-1 without non-indexed additional reflections (see Fig. 1 for examples and the ESI details). To get further insights into the real structures of the activated Eu@IFP-1 and Tb@IFP-1 samples, we performed a combination of electron microscopy (SEM) and electron dispersive X-ray spectroscopy (EDX). Eu-elemental mapping shows a homogenous distribution of Eu³⁺ for a Eu-content lower than 0.50 atom% (e.g. Eu@IFP-1c; Fig. S08 at ESI).

The Eu- and Tb-elemental mappings of EuTb@IFP-1b also indicate a uniform distribution of lanthanides (Fig. 2a). At higher Eu-contents, the SEM image and the Eu-elemental mapping revealed that additional microcrystals of Eu(HCOO)₃ were formed (e.g. for 1.04 atom% (Eu@IFP-1d), Fig. S08, ESI). This is also observed for the referring Eu/Tb co-doped materials. Elemental mapping of EuTb@IFP-1d depicts microcrystals of mixed EuTb(HCOO)₃ deposited on the surface of a IFP-1 crystal (Fig. 2b). It can be anticipated that this microscopic difference illustrates the border of homogenous doping of the pore system for EuTb@IFP-1b and inhomogeneous doping for EuTb@IFP-1d, as only the latter shows mixed EuTb(HCOO)₃ on the outside of the MOF crystals. The microscopic formation of the secondary phase can be attributed to the decomposition of DMF to formates. It is intriguing that the border of homogenous doping of the MOF cannot be observed by PXRD patterns of Ln@IPF-1, as the method is not suitable to determine very low amounts of secondary phases. Instead combination with other microscopic methods, as done here by SEM and EDX is essential for such modifications of MOFs in order to determine the correct character. Apparently, PXRD can only determine the reflections of Ln(HCOO)₃ at much higher concentrations. We therefore also carried out TG-MS measurements to identify the Ln(HCOO)₃ (see ESI for details). We selected some of these doped materials for the details of gas sorption and fluorescence studies.

Sorption and Porosity

In order to investigate the dependence of the doping with lanthanide ions on the microporosity of IFP-1, physisorption experiments were carried out with N₂ at 77 K on non-doped IFP-1 and frameworks homogeneously doped with Eu³⁺ (Eu@IFP-1c), Tb³⁺ (Tb@IFP-1d) and Eu³⁺ together with Tb³⁺ (EuTb@IFP-1b), as well as on MOF material showing the start of microscopic phase separation at a higher dopant degree by formation of EuTb(HCOO)₃ on the surface of EuTb@IFP-1d. For further comparison, sorption experiments were also carried out with CO₂ at 195 K on non-doped IFP-1 and Eu@IFP-1c.

Specific surface areas were estimated by the use of adsorption isotherms for both N₂ and CO₂ utilizing the Brunauer-Emmet-Teller model (BET).

Adsorption and desorption isotherms indicate microporosity for IFP-1, Eu@IFP-1c and Tb@IFP-1d of the same magnitude, for both N₂ and CO₂ sorption (Fig. 3). The full microporosity of the IFP-1 framework is retained upon doping with lanthanide ions, as long as no phase separation is observed (Table 2).

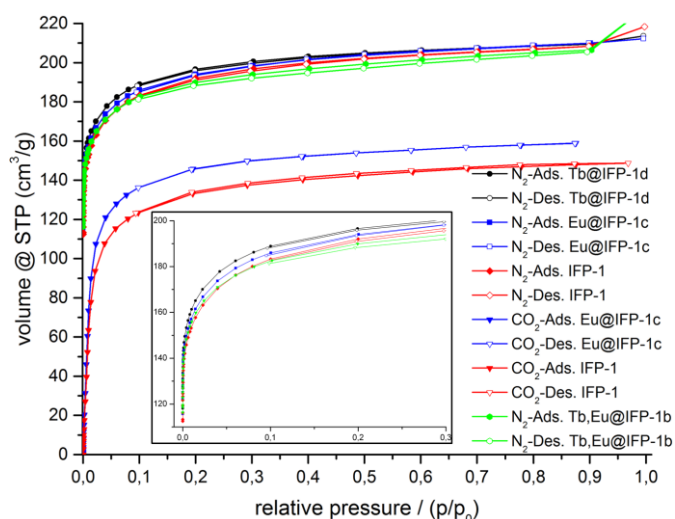


Fig. 3 Adsorption (closed symbols) and desorption isotherms (open symbols) for N₂ sorption at 77 K and CO₂ at 195 K on IFP-1, homogeneously doped Eu@IFP-1c, Tb@IFP-1d and EuTb@IFP-1b.

For dopant degrees lower than 0.50 atom% of Ln³⁺ ions, no blockage of pores is observed besides the equilibration hindrance, which should be a sign for homogenous doping that is not only on the outer surface of the MOF, as this would lead to blockage of pores and a loss or stronger reduction of the inner surface. Accordingly, the surface investigations also assume that Eu@IFP-1c, Tb@IFP-1d and EuTb@IFP-1b are homogeneously doped porous MOF phosphors. Observed deviations in the surface area between IFP-1 and Ln³⁺-doped IFP can mostly be addressed to influences of synthesis conditions. Hence, the in-situ loading of microporous IFP-1 can be successfully carried out without diminishing the porosity of the MOF.

Table 2. Calculated BET-surface areas and total pore volumes of IFP-1, Eu@IFP-1c, Tb@IFP-1d, EuTb@IFP-1b and EuTb@IFP-1d for N₂ and CO₂ adsorption.

Sample	Surface area(BET)	Total pore volume
N ₂ on IFP-1	737 m ² /g	0.33 cm ³ /g
N ₂ on Eu@IFP-1c	758 m ² /g	0.33 cm ³ /g
N ₂ on Tb@IFP-1d	745 m ² /g	0.33 cm ³ /g
N ₂ on EuTb@IFP-1b	702 m ² /g	0.31 cm ³ /g
N ₂ on EuTb@IFP-1d	633 m ² /g	0.28 cm ³ /g
CO ₂ on IFP-1	736 m ² /g	0.28 cm ³ /g
CO ₂ on Eu@IFP-1b	768 m ² /g	0.30 cm ³ /g

Non-doped IFP-1 shows a total uptake of 208 cm³g⁻¹ for N₂ and 148 cm³g⁻¹ for CO₂, while doped Eu@IFP-1c and Tb@IFP-

1d show total uptakes of 210 cm³g⁻¹ for N₂ each, as well as 159 cm³g⁻¹ of CO₂ on Eu@IFP-1c (at relative pressures close to unity). This indicates comparable inner surface areas for non-doped IFP-1 and all homogeneously low-doped frameworks investigated (Table 2) despite the different analyte temperatures.

For dopant concentrations higher than 1.00 atom% the gas uptake decreases, as the additional phases Ln(HCOO)₃ are deposited as microcrystals on the outer surface of the homogenous Ln-doped IFP. Even though on a μm scale, they are large enough to block channels of the pore system, as shown for EuTb@IFP-1d. This sealing-off of some part of MOF micropores reduces the inner surface and thus the gas uptake. For an amount of 14 atom% of Eu³⁺ and Tb³⁺ ions, as determined for EuTb@IFP-1d, the observed reduction of the specific surface area is about 14 %, equaling 104 cm³g⁻¹ and corresponding to a reduced specific surface area of 633 m²g⁻¹ for N₂. The option to achieve both, homogenous doping as well as phase separation further supports the idea that the pore system of IFP-1 can be utilized for doping, but that there are certain limits for the homogenous co-doping of IFP-1 with lanthanide ions.

Because of the chemical and thermal stability of the the intrinsic one-dimensional channel structure, the zinc constituted IFP-1 is also formed in the presence of nitrates of Eu³⁺ and Tb³⁺. It could be anticipated that the lanthanide ions are encapsulated into the channels of IFP-1 and not statistically substituting the connectivity centers, as there is a large mismatch between Zn²⁺ and Ln³⁺ in ionic radii and charge. Presence of the imidate and amide groups of the channel walls and thus the inner surface of IFP-1 enhances the polarization and hydrophilic character of the channels and allows interaction with lanthanide ions. Low-doped Ln@IFP-1 contains only small amounts of Ln³⁺ ions, which introduce an imbalance in the electronic equilibrium of the network that needs to be balanced by a corresponding amount of anions. Based on the analytics described above, we assume an additional intercalation of formate anions. Further electronic exchange for charge equilibration at functional groups is possible inside the channels of the framework.

Photoluminescence

Non-doped IFP-1 exhibits a weak photoluminescence due to a broad, blue emission band ranging from 375 nm to 700 nm at RT with its maximum at λ_{max} = 463 nm (λ_{ex} = 360 nm) (Fig. 4). The excitation band in the range of 300 nm to 425 nm is also broad with its maximum at λ_{max} = 355 nm (λ_{em} = 463 nm) and a shoulder around λ_{shoulder} ~ 430 nm (Fig. S13). Doping of the IFP framework by the in-situ available Eu³⁺ and Tb³⁺ ions during the formation reaction introduces additional luminescence properties. Besides the framework fluorescence, the lanthanide containing materials, e.g. Eu@IFP-1c and Tb@IFP-1d, exhibit additional, characteristic lanthanide emission bands.^{16,17} The additional emission bands originate from corresponding metal-centered 4f-4f transitions of the respective trivalent lanthanide ions in the Ln³⁺-doped IFP-1. The emission can be observed by

excitation of the framework ligands, which act as a sensitizer for the lanthanide ions establishing an antenna effect¹⁸ (Fig. 4), indicating an energy transfer between the IFP-backbone and the Ln³⁺-dopants. The direct excitation of the Ln³⁺ 4*f*-4*f* transitions is also possible (Fig. 5), but weak compared to the antenna effect. Accordingly, the excitation spectra of doped Eu@IFP-1*c* and Tb@IFP-1*d* are very similar to the excitation spectra of non-doped IFP-1 (Fig. S13 at ESI) because of the low extinction coefficients of the lanthanide ions compared to the framework backbone.

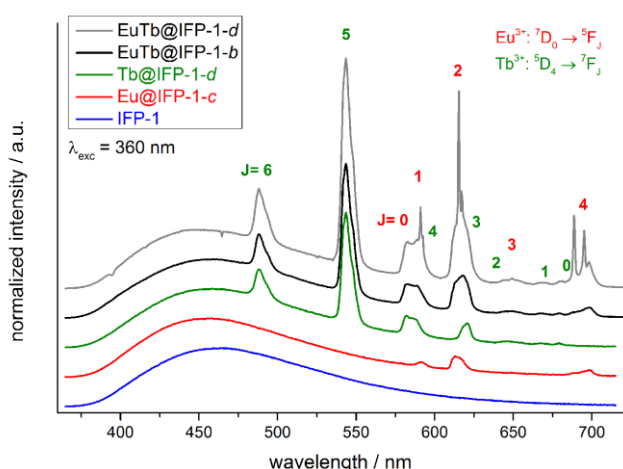


Fig. 4 Emission spectra of IFP-1, the homogeneously Ln³⁺-co-doped Eu@IFP-1*c*, Tb@IFP-1*d* and EuTb@IFP-1*b*, as well as the heterogeneously doped material EuTb@IFP-1*d* (all as-synthesized) obtained for indirect excitation conditions ($\lambda_{\text{exc}} = 360$ nm) at RT.

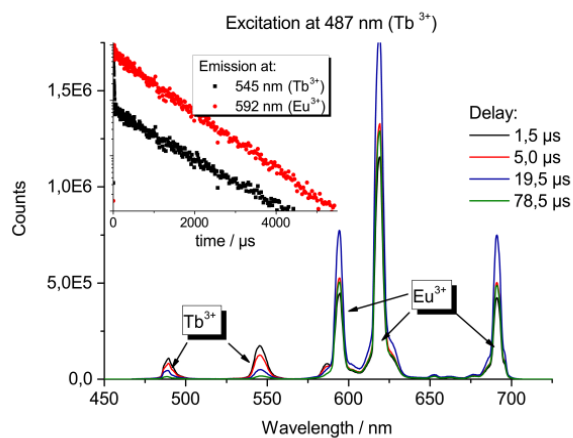


Fig. 5 Emission spectra of EuTb@IFP-1*d* (as synthesized) with the typical emission bands for Eu³⁺ and Tb³⁺ after direct excitation of Tb³⁺ at $\lambda_{\text{ex}} = 487$ nm recorded with different delays between excitation and emission measurement. The inset shows the emission decay kinetics for Tb³⁺ and Eu³⁺.

For Tb@IFP-1*d*, the typical Tb³⁺-transitions $^5D_4 \rightarrow ^7F_J$ ($J = 6-0$) are observed, and for Eu@IFP-1*c* the Eu³⁺-transitions $^5D_0 \rightarrow ^7F_J$ ($J = 0-4$) are detected. After introduction of the Eu³⁺ or Tb³⁺ ions to the framework, the intensity of the broad emission band of the framework itself does not change

significantly. Comparing the intensities of the sensitized Ln³⁺-emission, the Tb³⁺-containing compound Tb@IFP-1*d* shows a more intensive 4*f*-4*f* emission than Eu@IFP-1*c* (Fig. 4). Excitation of co-doped IFP with Eu³⁺ and Tb³⁺ (Fig. 4, EuTb@IFP-1*b* and EuTb@IFP-1*d*) leads to the blue framework emission along with the characteristic green and orange-red emissions of Tb³⁺ and Eu³⁺, respectively.

Framework backbone centered emission and Ln³⁺-centered emission can also be distinguished by investigations of the decay time of the photoluminescence processes. The decay time of the fluorescence process is on the low nanosecond scale for the broad band emission of the ligand (IFP-1: $\tau = 0.33(1) - 5.74(20)$ ns, Eu@IFP-1*c*: $\tau = 0.13(1) - 4.22(14)$ ns, Tb@IFP-1*d*: $\tau = 0.04(2) - 4.82(16)$ ns), which is much faster than the luminescence decay times found for Eu³⁺ and Tb³⁺ (Eu@IFP-1*c*: $\tau = 314(13) - 1337(117)$ μ s, Tb@IFP-1*d*: $\tau = 580(33) - 1062(60)$ μ s; see also Table S6).

In the Eu³⁺- and Tb³⁺-co-doped samples, in addition to the antenna effect of the ligand, a metal-to-metal energy transfer from Tb³⁺ to Eu³⁺ was detected for the materials EuTb@IFP-1*b* and EuTb@IFP-1*d*. This energy transfer is more effective for higher lanthanide loadings as the efficiency of the energy transfer depends on the average distances between donor and acceptor (Fig. 4). Given a random distribution of dopants the distance between Eu³⁺ and Tb³⁺ is inversely to the metal loading. The Tb³⁺ \rightarrow Eu³⁺ metal-to-metal energy transfer is proven by detection of Eu³⁺ emission after selective excitation of Tb³⁺ ($\lambda_{\text{ex}} = 478$ nm) and the observed luminescence decay kinetics of Tb³⁺ and Eu³⁺, as shown with site selective PL spectroscopy (Fig. 5). This energy transfer is a great tool to fine-tune the color point and thus the chromaticity of the white emitting materials. Higher Eu³⁺ emission intensities lead to a warmer white emission (vide infra).

White Light Emission Properties

As stated, the organic part of the framework contributes a broad band emission in the blue spectral range, Tb³⁺ and Eu³⁺ add a green and a red emission component, respectively, to the EuTb-co-doped IFP-1 materials. Altogether this enables the emission of white light by EuTb@IFP-1, as the materials (as shown for EuTb@IFP-1*b* and EuTb@IFP-1*d*) exhibit a combination of the framework fluorescence and the luminescence of Tb³⁺ as well as Eu³⁺ (Fig. 4 and 5). The three color emitter EuTb@IFP-1 thereby meets today's standards of color rendering of LED phosphors and exceeds the recent two color emitting MOFs.^{10,19} Compared to IFP-1 co-doped with one lanthanide ion, only, like Eu@IFP-1*b* and *d*, a significant increase in Eu³⁺-luminescence intensity is observed contributing to the overall white emission color of the materials EuTb@IFP-1*b* and EuTb@IFP-1*d* (Fig. 4 and 5). It is remarkable that EuTb@IFP-1 shows a tunable chromaticity point with varying dopant concentrations (Fig. 6 and Table S5).

In addition, also the temperature can be used to influence the color point of the materials. One reason is a reduction of the blue ligand emission upon increasing temperature. Consequently, the overall white color temperature of the co-

doped IFP is also temperature dependent (Fig. 6). At 77 K, EuTb@IFP-1*d* emits a cold white light, which turns into a warm white light at RT. Hence the warmth of the white color could also be used for temperature sensing, as recently shown for Eu_{0.0069}Tb_{0.9931}-DMBDC (DMBDC: 2,5-dimethoxy-1,4-benzene-dicarboxylate).^{11a} The color point is moved further to a warmer color by larger amounts of lanthanide ions. This behavior can be explained by smaller average Tb³⁺-Eu³⁺ distances and therefore a more effective metal-to-metal energy transfer leading to an increased contribution of the red Eu³⁺ emission to the white light (Fig. 6). It is intriguing that besides the homogenous distribution of the lanthanide ions in the pore system, also heterogeneous composites of EuTb@IFP-1 with lanthanide formate crystals on the outer surface can have beneficial effects on the tuning of the warmth of the white light emission. This further underlines the importance to distinguish between homogenous loading of the pore system of the MOF and a utilization of the outer surface for an understanding of the processes observed.

In order to understand the coordination environment and position of Ln³⁺-dopants incorporated into the IFP materials during synthesis, high resolution Eu³⁺-spectra were recorded. At ultra-low temperatures of 4 K, processes contributing to the spectral broadening of electronic transitions (inhomogeneous broadening) are minimized and small differences in the electronic spectra of different chemical species or chemical species in different environments and coordination can be resolved. Site selective Eu³⁺-spectroscopy using a narrow bandwidth dye laser as excitation light source offers a unique possibility to probe Eu³⁺ ions and distinguish their different chemical environments. Due to the non-degenerate ground (⁷F₀) and first excited states (⁵D₀) of Eu³⁺, the corresponding electronic transition of a single species of Eu³⁺ ions consists of only one peak which is not split by the crystal field. The energy of the absorption and emission is dependent on the strength of the crystal field and differs for different Eu³⁺ species (nephelauxetic effect). Subsequently, different chemical species present in one single sample can be probed individually. Moreover, the obtained Stark-splitting patterns of the lower energy transitions ⁵D₀→⁷F₁-⁷F₆ contain complementary information on the individual chemical species, e.g., the symmetry and homogeneity of a distinct lattice site. We chose different Eu@IFP-1 samples to elaborate the study on the location and coordination environment of the lanthanide ions.

Homogeneously doped Eu@IFP-1*b* and EuTb@IFP-1*b* (both as-synthesized) show no sharp, distinct emission lines indicating that the probed Eu³⁺ ions are located in non-homogeneous binding environments (Fig. 7) and not on a distinct crystallographic site, if they replaced the connectivity centers of IFP-1. The broad, unresolved luminescence originates from Eu³⁺ ions distributed over a variety of slightly different chemical environments in the sample, which would be possible inside the pores of the MOF. Based on the luminescence spectra no indication of a separate phase including formate is found, which is in good agreement with

the other analytical results (Fig. S08b at ESI and 2a, respectively).

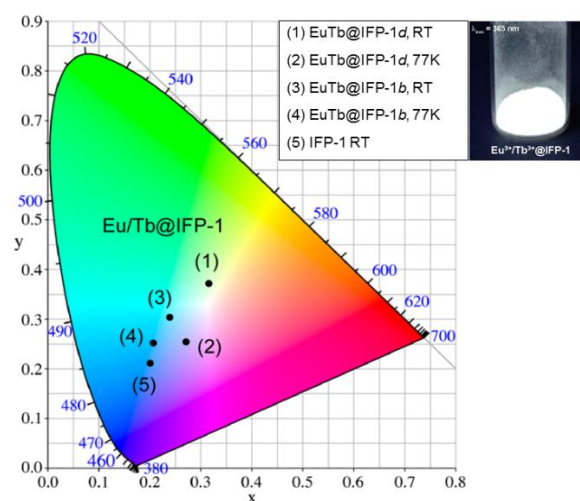


Fig. 6 Chromaticity diagram of as-synthesized EuTb@IFP-1*b* and EuTb@IFP-1*d* at room temperature and at 77 K illustrating the dependence of the temperature on the chromaticity point according to CIE and visual impression of the white emission of as-synthesized EuTb@IFP-1*d*.

Site-selective excitation of the ⁵D₀→⁷F₀ transition of the various doped Eu@IFP-1*d* and EuTb@IFP-1*d* (both as synthesized) yielded luminescence spectra showing one Eu³⁺ species with a two-fold crystal field splitting of the ⁵D₀-⁷F₁ and ⁵D₀-⁷F₂ transitions along with the same broad luminescence without well-resolved Stark-splitting (Fig. 7).

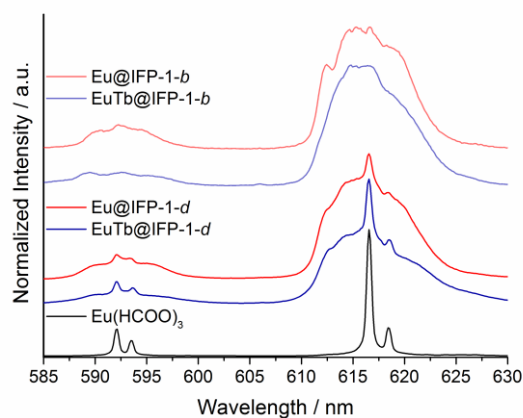


Fig. 7 Emission spectra of Eu(HCOO)₃, homogenous/heterogeneous Ln³⁺ co-doped Eu@IPF-1*d* and EuTb@IPF-1*d*, as well as homogenous doped Eu@IFP-1*b* and EuTb@IPF-1*b* (all as-synthesized) after excitation at $\lambda_{\text{ex}} = 579.60$ nm, the excitation maximum of Eu(HCOO)₃. All spectra are extracted from the total luminescence spectra (as shown in Figure 6) after a scan over the ⁷F₀-⁵D₀ transition at T = 4 K.

Comparison with a Eu(HCOO)₃ reference shows that the sharp, two-fold split luminescence lines can be attributed to the formation of small domains of crystalline Eu(HCOO)₃. This again is in very good agreement with the results obtained from

SEM and EDX (Fig. S08d) and shows that the region of homogenous doping can also be spectroscopically identified by ultra-low temperature PL spectroscopy.

Removal of solvent molecules by heating the Eu@IFP-1*d* samples to 200 °C in a vacuum of 1 mbar was performed until the sample mass was constant. In the total emission spectra (Fig. 8) two things can be seen: i) the sharp emission peaks attributed to the formate phase ($\lambda_{\text{ex}} = 579.6$ nm, vide supra) are preserved and ii) alteration in shape / structure of the broad excitation and emission bands (Fig. 8). Alterations in the spectra always originate from alterations in the crystal field experienced by the Eu^{3+} -dopants. The changes in the broad excitation and emission bands suggest that the Eu^{3+} ions are located inside the channels of IFP-1 from which the solvent escapes, as opposed to an additional (formate) phase and/or the outside surface of the MOF. The changes in the luminescence signature upon removal of solvent molecules from the MOF framework channels, at the same time, strongly supports the previously concluded saturation of the coordination spheres of Eu^{3+} by solvent molecules.

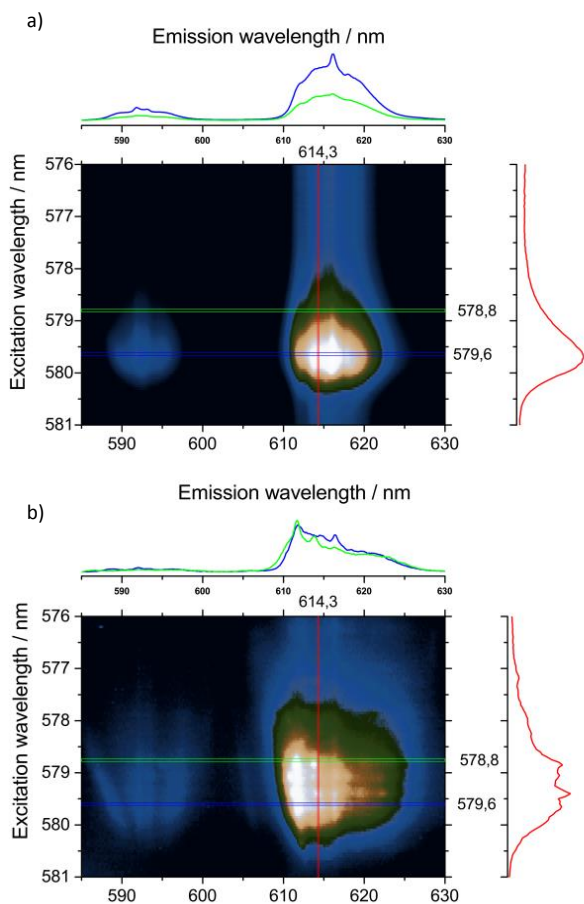


Fig. 8 Total emission spectra (logarithmic intensity/color scale) of Eu@IPF-1*d* (as-synthesized (top) and activated (bottom)) after excitation of the ${}^7\text{F}_0\text{-}{}^5\text{D}_0$ transition between $\lambda_{\text{ex}} = 576 - 581$ nm at $T = 4$ K. Note the formate peak at $\lambda_{\text{em}} = 616.2$ nm and the excitation and emission broadening in the activated sample due to increased general inhomogeneity of the coordination spheres of the dopant ions.

Although the emission and excitation bands appear overall broadened upon the removal of solvent molecules indicating greater variations in the crystal fields, the increased structure in the emission and excitation spectra is clearly visible. The structure in the spectra can be interpreted as more distinct, more crystalline-like crystal sites, where greater numbers of Eu^{3+} ions have very similar coordination spheres and therefore crystal fields.

The colored intensity plots of the total luminescence allow a rough estimation of the number of different lattice sites, meaning groups of Eu^{3+} -dopants experiencing an identical crystal field. About four groups of identical Eu^{3+} ions can be excited in a very narrow bandwidth between 578.8 nm and 579.6 nm for the activated samples, each group showing different emission intensity patterns (Fig. 8b). It seems, due to the relatively rigid structure of the MOF, that there is a limited amount of symmetries that can stabilize the depleted coordination spheres of Eu^{3+} -dopants after removal of solvent molecules, thus explaining the sharpened peaks. This indicates favored positions of the Ln^{3+} ions within the pore system, interacting with the functional groups of the linker. Trapping of Eu^{3+} and Tb^{3+} ions was just recently shown for the MOF $\text{Zn}_4\text{O}(\text{L})_{1.5}$, $\text{L} = 6,6'-(2,2\text{-bis}((6\text{-carboxy-naphthalen-2-yl}oxy)methyl)propane-1,3\text{-diyl})bis(oxy)di-2\text{-naphthoate}$ showing a color tuning of the luminescence from green to red at different Eu/Tb ratios.^{20a} Capture of Ln^{3+} -ions in MOF pores was also used for the detection of Ln^{3+} by uptake of the ions Eu^{3+} and Tb^{3+} into IFMC, a zinc nitrate MOF with tricarboxylate ligands based on a central tripodal ether group, to give Eu@IFMC-10 and Tb@IFMC-10.^{20b}

For EuTb@IFP-1, indirect excitation of europium in the UV spectral range using framework sensitization supports the interpretation that the unstructured, broad emission is caused by Ln^{3+} ions located inside the channels of the MOF material. The antenna effect depends on the close proximity of metal ion and the sensitizer (MOF channel walls coordinating Ln^{3+}). Thereby, site selective photoluminescence spectroscopy and total emission spectra give vital insights into the nature of the lanthanide uptake in the pores and also corroborate the formation of lanthanide formate side phases from a certain Ln-amount on, as the luminescence of both phenomena can be clearly distinguished.

Conclusions

To summarize, the formation of a white light emitting MOF is achieved by simultaneous co-doping of IFP-1 with Tb^{3+} and Eu^{3+} during the in-situ formation of the ligand and the MOF. This in-situ co-doping with trivalent Ln^{3+} ions enables luminescent MOFs with almost identical porosity as the non-doped framework. The three emission colors blue, green and red are thereby combined in one emitter. The luminescence of the IFP-1 backbone together with 4f-emission of the lanthanide ions add to a three-color white light emitting MOF that expands to the efforts of previously known one- and two-color white emitters. The photoluminescence is supported by ligand-to-

metal and metal-to-metal energy transfers, the color of the white light emission being temperature and Ln^{3+} concentration dependent. A more bluish chromaticity is observed for cooling to 77 K and for low dopant degrees, whereas a warmer white light is emitted at RT for high dopant amounts. This effect can be potentially used for a spectroscopic temperature sensing. The lanthanide ions do not replace zinc ions as connectivity centers but are intercalated into the pore system of the IFP-1 MOF during synthesis without a structure directing effect. The uptake is homogenous with no detectable differences in distribution if the final dopant degree is lower than 1.0 atom% referred to the amount of Zn^{2+} . At higher dopant degrees, phase formation of lanthanide formates from decomposition of the solvent DMF starts to occur in addition to the intercalation into the MOF. The lanthanide formates can be characterized as secondary crystalline phase at the outer surface of the MOF particles and limit the homogenous region of co-doping. Intercalated Ln^{3+} ions and lanthanide formates can be clearly distinguished by means of photoluminescence spectroscopy, SEM/EDX and sorption experiments. Eu- and Tb-formates on the surface can be beneficially used to further tune the chromaticity of the MOF in a composite relation. The luminescent MOFs Ln@IFP-1 retain their microporosity upon loading with luminescence centers regarding sorption of N_2 at 77 K and CO_2 at 195 K in the homogenous region of co-doping. To the best of our knowledge, EuTb@IFP-1d is the first example of a white light emitting MOF with proven porosity in combination with luminescence centers inside the pore system and not substituting connectivity centers of the MOF.

Acknowledgements

The authors thank Dr. C. Günter (Universität Potsdam) for help with X-ray powder diffraction measurements, Dr. M. Neumann for TG-MS measurements, S. Lubahn (Universität Potsdam) for the ICP-OES measurements and Y. Linde (Universität Potsdam) for the C, H, N elemental analysis. This work is financially supported by the Priority Program 1362 of the German Research Foundation on "Metal–Organic Frameworks" and the Dr. Klaus-Römer foundation.

Notes and references

^a Institut für Chemie, Anorganische Chemie, Universität Potsdam, Karl-Liebknecht-Straße 26, 14476 Golm, Germany

^b Institut für Anorganische Chemie, Universität Würzburg, Am Hubland, 97074 Würzburg, Germany

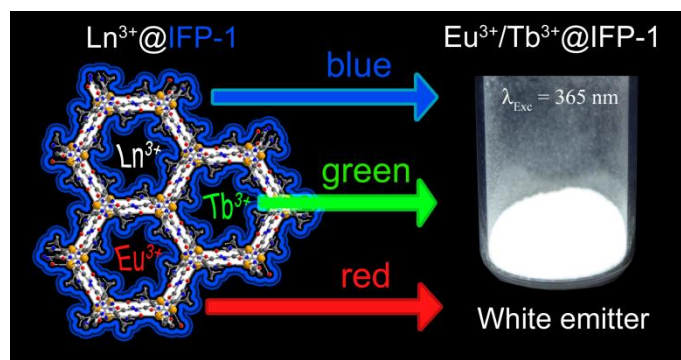
^c Institut für Chemie, Physikalische Chemie, Universität Potsdam, Karl-Liebknecht-Str. 25, 14476 Golm, Germany

† Electronic Supplementary Information (ESI) available: [details of IR-spectroscopy, Elemental analysis, ICP-OES, powder X-ray diffraction, Scanning electron microscopy, Energy-dispersive X-ray spectroscopy, Thermogravimetric analysis, TG-MS, gas sorption, photoluminescence and decay investigations]. See DOI: 10.1039/b000000x/

- (a) J. L. C. Rowsell and O. M. Yaghi, *Microporous Mesoporous Mater.* 2004, **73**, 3; (b) O. M. Yaghi and G. Li, H. Li, *Nature* 1995, **378**, 703; (c) G. J. Férey, C. Mellot-Draznieks, C. Serre and F. Millange, *Acc. Chem. Res.*, 2005, **38**, 217; (d) S. L. James, *Chem. Soc. Rev.*, 2003, **32**, 276; (e) S. Meek, J. Greathouse and M. Allendorf, *Adv. Mater.* 2011, **23**, 249; (f) M. Li, D. Li, M. O'Keeffe and O. M. Yaghi, *Chem. Rev.*, 2014, **114**, 1343.
- (a) S. Ma and H.-C. Zhou, *Chem. Commun.*, 2010, **46**, 44; (b) K. Sumida, D. L. Rogow, J. A. Mason, T. M. McDonald, E. D. Bloch, Z. R. Herm, T.-H. Bae and J. R. Long, *Chem. Rev.*, 2012, **112**, 724; (c) M. P. Suh, H. J. Paark, T. K. Prasad and D.-W. Lim, *Chem. Rev.*, 2012, **112**, 782; (d) L. J. Murray, M. Dincă and J. R. Long, *Chem. Soc. Rev.*, 2009, **38**, 1294; (e) A. U. Czaja, N. Trukhan and U. Müller, *Chem. Soc. Rev.*, 2009, **38**, 1284; (f) T. R. Cook, Y.-R. Zheng and P. J. Stang, *Chem. Rev.*, 2013, **113**, 734.
- (a) L. Pan, D. H. Olson, L. R. Ciemnomolonski, R. Heddy and J. Li, *Angew. Chem. Int. Ed.*, 2006, **45**, 616; (b) J.-R. Li, J. Sculley and H.-C. Zhou, *Chem. Rev.*, 2012, **112**, 869; (c) J.-R. Li, R. J. Kuppler and H.-C. Zhou, *Chem. Soc. Rev.*, 2009, **38**, 1477.
- (a) A. M. Shultz, O. K. Farha, J. T. Hupp and S. T. Nguyen, *J. Am. Chem. Soc.*, 2009, **131**, 4204; (b) D. J. Lun, G. I. N. Waterhouse and S. G. Telfer, *J. Am. Chem. Soc.*, 2011, **133**, 5806; (c) R. E. Morris and X. Bu, *Nature Chem.* 2010, **2**, 353.
- (a) X. L. Qi, R. B. Lin, Q. Chen, J. B. Lin, J.-P. Zhang and X.-M. Chen, *Chem. Sci.*, 2011, **2**, 2214; (b) Y.-N. Wu, F. Li, W. Zhu, J. Cui, C.-A. Tao, C. Lin, P. M. Hannam and G. Li, *Angew. Chem. Int. Ed.*, 2011, **50**, 12518.
- (a) P. Horcajada, C. Serre, M. Vallet-Regi, M. Sebban, F. Taulelle and G. J. Férey, *Angew. Chem. Int. Ed.*, 2006, **45**, 5974; (b) P. Horcajada, C. Serre, G. Maurin, N. A. Ramsahye, F. Balas, M. Vallet-Regi, M. Sebban, F. Taulelle and G. J. Férey, *J. Am. Chem. Soc.*, 2008, **130**, 6774; (c) S. Keskin and S. Kizilel, *Ind. Eng. Chem. Res.*, 2011, **50**, 1799.
- (a) Z. Hu, B. J. Deibert and J. Li, *Chem. Soc. Rev.*, 2014, **43**, 5815; (b) Q.-Y. Liu, Y.-L. Wang, N. Zhang, Y.-L. Jiang, J.-J. Wie and F. Luo, *Cryst. Growth Des.*, 2011, **11**, 3717; (c) K. Liu, H. You, Y. Zheng, G. Jia, L. Zhang, Y. Huang, M. Yang, Y. Song and H. Zhang, *CrystEng. Comm.*, 2009, **11**, 2622; (d) H. Zhang, N. Li, C. Tian, T. Liu, F. Du, P. Lin, Z. Li and S. Du, *Cryst. Growth Des.*, 2012, **12**, 670; (e) C. J. Höller, M. Mai, C. Feldmann and K. Müller-Buschbaum, *Dalton Trans.*, 2010, **39**, 461.
- (a) M. D. Allendorf, C. A. Bauer, R. K. Bhakta and R. J. T. Houk, *Chem. Soc. Rev.*, 2009, **38**, 1330; (b) J. Rocha, L. D. Carlos, F. A. Almeida Paz and D. Ananias, *Chem. Soc. Rev.*, 2011, **40**, 926; (c) Y. Cui, Y. Yue, G. Qian and B. Chen, *Chem. Rev.*, 2012, **112**, 1126; (d) N. Stock and S. Biswas, *Chem. Rev.*, 2012, **112**, 933; (e) J. Heine and K. Müller-Buschbaum, *Chem. Soc. Rev.*, 2013, **42**, 9232; (f) Z. Hu and B. J. Deibert, J. Li, *Chem. Soc. Rev.*, 2014, **43**, 5815; (g) Y. Cui, B. Chen and G. Qian, *Coord. Chem. Rev.*, 2014, **273**, 76; (h) J. Lei, R. Qian, P. Ling, L. Cui and H. Ju, *Trends Analyt. Chem.*, 2014, **58**, 71; (i) C. Dey, T. Kundu, B. P. Biswal, A. Mallick and R. Banerjee, *Acta Cryst.*, 2014, **B70**, 3; (j) D. Liu, K. Lu, C. Poon and W. Lin, *Inorg. Chem.*, 2014, **53**, 1916; (k) Y. F. Chen, Y.-C. Ma and S.-M. Chen, *Cryst. Growth Des.*, 2013, **13**, 4154.
- (a) P. Falcaro and S. Furukawa, *Angew. Chem.*, 2012, **51**, 8431; (b) A. Zurawski, M. Mai, D. Baumann, C. Feldmann and K. Müller-Buschbaum, *Chem. Commun.*, 2011, **47**, 496; (c) P. R. Matthes, C. J. Höller, M. Mai, J. Heck, S. J. Sedlmaier, S. Schmiechen, C.

- Feldmann, W. Schnick and K. Müller-Buschbaum, *J. Mater. Chem.*, 2012, **22**, 10179; (d) Q. Tang, S. Liu, Y. Liu, D. He, J. Miao, X. Wang, Y. Ji and Z. Zheng, *Inorg. Chem.*, 2014, **53**, 289; (e) V. Haquin, M. Etienne, C. Daiguebonne, S. Freslon, G. Calvez, K. Bernot, L. Le Pollès, S. E. Ashbrook, M. R. Mitchell, J.-C. Bünzli, S. V. Eliseeva and O. Guillou, *Eur. J. Inorg. Chem.*, 2013, 3464; (f) H. Zhang, X. Shan, L. Zhou, P. Lin, R. Li, E. Ma, X. Guoab and S. Du, *J. Mater. Chem. C*, 2013, **1**, 888; (g) J.-C. Rybak, M. Hailmann, P. R. Matthes, A. Zurawski, J. Nitsch, A. Steffen, J. G. Heck, C. Feldmann, S. Götzendörfer, J. Meinhardt, G. SEXTL, H. Kohlmann, S. J. Sedlmaier, W. Schnick and K. Müller-Buschbaum, *J. Am. Chem. Soc.*, 2013, **135**, 6896; (h) H. Zhang, X. Shan, Z. Ma, L. Zhou, M. Zhang, P. Lin, S. Hu, E. Ma, R. Li and S. Du, *J. Mater. Chem. C*, 2014, **2**, 1367; (i) Y. Wang, Y.-Y. Liu and J.-F. Ma, *Chem. Eur. J.*, 2013, **19**, 14591.
- 10 D. F. Sava, L. E. S. Rohwer, M. A. Rodriguez and T. M. Nenoff, *J. Am. Chem. Soc.*, 2012, **134**, 3983.
- 11 (a) Q. Tang, S. Liu, Y. Liu, D. He, J. Miao, X. Wang, Y. Ji, Z. Zheng, *Inorg. Chem.*, 2014, **53**, 289; (b) A. Ablet, S.-M. Li, W. Cao, X.-J. Zheng, W.-T. Wong and L.-P. Jin, *Chem. Asian J.*, 2013, **8**, 95; (c) Y. Liu, M. Pan, Q.-Y. Yang, L. Fu, K. Li, S.-C. Wei and C.-Y. Su, *Chem. Mater.*, 2012, **24**, 1954; (d) F. Luo, M.-S. Wang, M.-B. Luo, G.-M. Sun, Y.-M. Song, P.-X. Lia and G.-C. Guo, *Chem. Commun.*, 2012, **48**, 5989; (e) C.-Y. Sun, X.-L. Wang, X. Zhang, C. Qin, P. Li, Z.-M. Su, D.-X. Zhu, G.-G. Shan, K.-Z. Shao, H. Wu and J. Li, *Nat. Comm.*, 2013, **4**, 2717; (f) R. V. Meyer, F. Schönfeld and K. Müller-Buschbaum, *Chem. Commun.*, 2014, **50**, 8093.
- 12 (a) S. P. Nakamura, *Soc. Photo-Opt. Ins.*, 1997, **3002**, 26; (b) R. Mueller-Mach, G. O. Mueller, M. R. Krames and T. Trotter, *IEEE J. Sel. Top Quant.*, 2002, **8**, 339.
- 13 (a) R. Mueller-Mach, G. O. Mueller, M. R. Krames, H. A. Hoppe, F. Stadler, W. Schnick, T. Juestel and P. Schmidt, *Phys. Status Solidi A*, 2005, **202**, 1727; (b) E. F. Schubert, *Light-emitting diodes*: Cambridge; New York: Cambridge University Press, 2006; (c) V. Bachmann, C. Ronda, O. Oeckler, W. Schnick and A. Meijerink, *Chem. Mater.*, 2009, **21**, 316; (d) T. Nägele, *LED Professional Rev.*, 2008, **10**, 1; (e) W. Lv, Y. Jia, Q. Zhao, W. Lü, M. Jiao, B. Shao and H. You, *J. Phys. Chem C*, 2014, **118**, 4649; (f) Y. Zhang, D. Geng, X. Li, J. Fan, K. Li, H. Lian, M. Shang and J. Lin, *J. Phys. Chem. C*, 2014, **118**, 17983; (g) G. Li, C. C. Lin, W.-T. Chen, M. S. Molokeev, V. V. Atuchin, C.-Y. Chiang, W. Zhou, C.-W. Wang, W.-H Li, H. S.; Sheu, T.-S. Chan, C. Ma and R.-S. Liu, *Chem. Mater.*, 2014, **26**, 2991.
- 14 (a) F. Debatin, A. Thomas, A. Kelling, N. Hedin, Z. Bacsik, I. Senkovska, S. Kaskel, M. Junginger, H. Müller, U. Schilde, C. Jäger, A. Friedrich and H.-J. Holdt, *Angew. Chem. Int. Ed.*, 2010, **49**, 1258; (b) F. Debatin, K. Behrens, J. Weber, I. A. Baburin, A. Thomas, J. Schmidt, I. Senkovska, S. Kaskel, A. Kelling, N. Hedin, Z. Bacsik, S. Leoni, G. Seifert, C. Jäger, C. Günter, U. Schilde, A. Friedrich and H.-J. Holdt, *Chem. Eur. J.*, 2012, **18**, 11630; (c) F. Debatin, J. Möllmer, S. S. Mondal, K. Behrens, A. Möller, R. Staudt, A. Thomas and H.-J. Holdt, *J. Mater. Chem.*, 2012, **22**, 10221; (d) S. S. Mondal, A. Bhunia, I. A. Baburin, C. Jäger, A. Kelling, U. Schilde, G. Seifert, C. Janiak and H.-J. Holdt, *Chem. Commun.*, 2013, **49**, 7599; (e) S. S. Mondal, S. Dey, I. A. Baburin, A. Kelling, U. Schilde, G. Seifert, C. Janiak and H.-J. Holdt, *CrystEngComm.*, 2013, **15**, 9394; (f) S. S. Mondal, A. Bhunia, S. Demeshko, A. Kelling, U. Schilde, C. Janiak, H.-J. Holdt, *CrystEngComm.*, 2014, **16**, 39; (g) S. S. Mondal, A. Bhunia, A. Kelling, U. Schilde, C. Janiak and H.-J. Holdt, *Chem. Commun.*, 2014, **50**, 5441.
- 15 (a) Y.-Q. Sun, J. Zhang, Y.-M. Chen and G.-Y. Yang, *Angew. Chem. Int. Ed.*, 2005, **44**, 5814; (b) Y.-Q. Sun, J. Zang and G.-Y. Yang, *Chem. Commun.*, 2006, **42**, 4700; (c) S.-R. Zheng, S.-L. Cai, Q.-Y. Yang, T.-T. Xia, J. Fan and W.-G. Zhang, *Inorg. Chem. Commun.*, 2011, **14**, 826; (d) Z.-H. Zhang, T.-A. Okamura, Y. Hasegawa, H. Kawaguchi, L. Y. Kong, W.-Y. Sun and N. Ueyama, *Inorg. Chem.*, 2005, **44**, 6219; (e) S.-M. Li, X. J. Zheng, D.-Q. Yuan, A. Ablet and L.-P. Jin, *Inorg. Chem.*, 2012, **51**, 1201; (f) R.-L. Chen, X.-Y. Chen, S.-R. Zheng, J. Fan and W.-G. Zhang, *Cryst. Growth Des.*, 2013, **13**, 4428; (g) Q. Tang, S. Liu, Y. Liu, D. He, J. Miao, X. Wang, Y. Ji and Z. Zheng, *Inorg. Chem.*, 2014, **53**, 289.
- 16 (a) J.-C. G. Bünzli and S. V. Eliseeva, *Basics of Lanthanide Photophysics*, in Springer Series on Fluorescence: Lanthanide Luminescence: Photophysical, Analytical and Biological Aspects, ed. O. S. Wolfbeis and M. Hof, vol. 7, Springer Verlag, Berlin, 2011; (b) G. H. Dieke, *Spectra and energy levels of rare earth ions in crystals*, Interscience Publishers, New York 1968.
- 17 (a) J.-C. G. Bünzli and C. Piguet, *Chem. Soc. Rev.*, 2005, **34**, 1048; (b) K. Binnemans, *Chem. Rev.*, 2009, **109**, 4283; (c) S. V. Eliseeva and J.-C. G. Bünzli, *Chem. Soc. Rev.*, 2010, **39**, 189.
- 18 (a) G. F. de Sá, O. L. Malta, C. de Mello Donegá, A. M. Simas, R. L. Longo, P. A. Santa-Cruz and E. F. da Silva Jr., *Coord. Chem. Rev.*, 2000, **196**, 165; (b) F. R. Gonçalves e Silva, O. L. Malta, C. Reinhard, H.-U. Güdel, C. Piguet, J. E. Moser and J.-C. G. Bünzli, *J. Phys. Chem. A*, 2002, **106**, 1670; (c) H. Guo, Y. Zhu, S. Qiu, J. A. Lercher and H. Zhang, *Adv. Mater.*, 2010, **22**, 4190.
- 19 A. Ablet, S.-M Li, W. Cao, X.-J. Zheng, W.-T. Wong and L.-P. Jin, *Chem. Asian J.*, 2013, **8**, 95.
- 20 (a) Y.-Q. Lan, H.-L. Jiang, S.-L. Li and Q. Xu, *Adv. Mater.*, 2011, **23**, 5015; (b) L. Chen, K. Tan, Y.-Q. Lan, S.-L. Li, K.-Z. Shao and Z.-M. Su, *Chem. Commun.*, 2012, **48**, 5919.

A graphical and textual abstract



A three color white light emitting microporous MOF with temperature and dopant dependent chromaticity is achieved by in-situ ligand plus framework formation and co-doping of IFP-1 with lanthanide ions. The microporosity and structure are retained upon intercalation of dopant luminescence centers into the pore system of the MOF.